

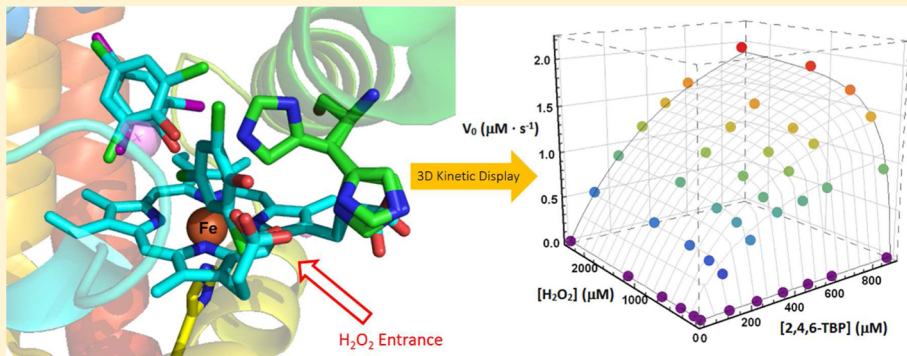
Distinct Enzyme–Substrate Interactions Revealed by Two Dimensional Kinetic Comparison between Dehaloperoxidase-Hemoglobin and Horseradish Peroxidase

Jing Zhao,[†] Chang Lu,[‡] and Stefan Franzen^{*,†,‡}

[†]Department of Chemistry, North Carolina State University, Raleigh, North Carolina 27695, United States

[‡]Department of Chemistry, Zhejiang University, Hangzhou, Zhejiang 310027, China

Supporting Information



ABSTRACT: The time-resolved kinetics of substrate oxidation and cosubstrate H_2O_2 reduction by dehaloperoxidase-hemoglobin (DHP) on a seconds-to-minutes time scale was analyzed for peroxidase substrates 2,4,6-tribromophenol (2,4,6-TBP), 2,4,6-trichlorophenol (2,4,6-TCP), and ABTS. Substrates 2,4,6-TBP and 2,4,6-TCP show substrate inhibition at high concentration due to the internal binding at the distal pocket of DHP, whereas ABTS does not show substrate inhibition at any concentration. The data are consistent with an external binding site for the substrates with an internal substrate inhibitor binding site for 2,4,6-TBP and 2,4,6-TCP. We have also compared the kinetic behavior of horseradish peroxidase (HRP) in terms of k_{cat} , $K_m^{\text{AH}_2}$ and $K_m^{\text{H}_2\text{O}_2}$ using the same kinetic scheme. Unlike DHP, HRP does not exhibit any measurable substrate inhibition, consistent with substrate binding at the edge of heme near the protein surface at all substrate concentrations. The binding of substrates and their interactions with the heme iron were further compared between DHP and HRP using a competitive fluoride binding experiment, which provides a method for quantitative measurement of internal association constants associated with substrate inhibition. These experiments show the regulatory role of an internal substrate binding site in DHP from both a kinetic and competitive ligand binding perspective. The interaction of DHP with substrates as a result of internal binding actually stabilizes that protein and permits DHP to function under conditions that denature HRP. As a consequence, DHP is a tortoise, a slow but steady enzyme that wins the evolutionary race against the HRP-type of peroxidase, which is a hare, initially rapid, but flawed for this application because of the protein denaturation under the conditions of the experiment.

INTRODUCTION

Dehaloperoxidase-hemoglobin (DHP) has had a controversial history that has led to the hypothesis that it is a true multi-functional enzyme. In 1977, DHP was characterized as a hemoglobin responsible for oxygen transport in the marine worm *Amphitrite ornata*.¹ In 1996, DHP was discovered to possess a peroxidase function because it can catalyze the oxidative dehalogenation reaction for 2,4,6-TBP and other phenolic substrates in the presence of cosubstrate H_2O_2 .² Upon examination, there is an apparent contradiction between globin and peroxidase functions³ that has been resolved by studies of function switching.^{4–6} Recently, DHP was also found to be a peroxygenase for a series of halogenated indole derivatives, which further expands its functional range.⁷ DHP even has significant oxidase activity, which brings the total number of

functions to four. As each of these functions has been discovered, there has been a normal skepticism regarding the significance of the reactivity for function in the living organism. There are many known adventitious heme enzyme functions that may not be true functions in an organism. For example, the bacterial hemoglobin from *Vitreoscilla* shows peroxidase activity similar to that of HRP,⁸ and it has been known for many years that human hemoglobin (Hb) is a better peroxidase than human myoglobin (Mb), but no physiological role for this activity is known.^{9,10} Sperm whale Mb has been the subject of significant protein engineering, leading to significant peroxidase

Received: July 22, 2015

Revised: September 8, 2015

Published: September 16, 2015

and peroxygenase activity in certain mutants.^{11–13} Although myoglobins can be engineered to have moderately high peroxidase activity, they are not competitive with functional peroxidases. Because the moderately high peroxidase activity of human Hb is thought to have no relevance for normal function in humans, it is natural to question whether the peroxidase function of DHP is functionally relevant in *A. ornata*.¹⁴

A proof of physiologically relevant function is a difficult task; however, the existence of multiple internal inhibitor binding sites in the heme distal pocket of DHP has provided evidence that DHP has evolved in ways that are unique within the globin family.^{15–21} These binding sites have no precedent in either the globin or the peroxidase protein family and suggest that the various toxins in the environment inhabited by *A. ornata* have specific differentiated interactions with DHP.²² The internal phenol binding sites also have structural relevance because they apparently increase the resistance of DHP to denaturation under certain conditions.²³ Because phenols are usually considered denaturants, this property combined with the catalytic rate suggests that DHP plays a unique role as a detoxification enzyme in *A. ornata*. Thus, continued exploration of the interaction of inhibitor binding and enzyme kinetics provides further evidence that the substrate interactions in DHP are not adventitious, but rather indicative of a true function. The rationale for this behavior is that detoxification is a sufficiently high priority for the organism that the various functions that eliminate toxins may have evolved in the Hb because it is the most abundant protein in the organism.¹⁰

The ping-pong mechanism is a name given to the two-electron oxidation of substrates via two subsequent one-electron steps in peroxidase enzymes.²⁴ This mechanism is considered to be a hallmark of peroxidase function.²⁵ In this study, we use a two-dimensional Michaelis–Menten model for H₂O₂ and substrate concentration to establish that DHP is a peroxidase that competes favorably with HRP at pH 7 specifically for oxidation of 2,4,6-TBP, which is considered to be the native substrate.^{2,21} 2,4,6-TCP has also been studied as a substrate because of its higher solubility. Therefore, it will be convenient to refer to both halogenated substrates using the designation 2,4,6-TXP (X = Cl, Br). Previous studies made the comparison at pH 5^{26,27} because HRP is a secretory peroxidase that has optimal reactivity at the low pH values found in the external environment.²⁸ The present study of the peroxidase mechanism in DHP and HRP at pH 7 clarifies the significance of that function in a multifunctional enzyme *in vivo*.

The evidence that DHP is a multifunctional enzyme can be found in the observation of several distinct substrate binding sites in DHP.^{15–21,29,30} The evidence for multiple binding sites can be divided into internal sites (X-ray crystallography, NMR,^{15–21,30} and flow-EPR, kinetics).²⁹ The first X-ray crystal structure of DHP showed that 4-iodophenol (4-IP) binds internally in the distal pocket above the heme.²¹ The aromatic ring is placed perpendicular to the heme plane offset from the iron atom toward the β -edge. Because of this structure, which was one of the first two structures published,²¹ DHP was believed to have an internal substrate binding site that undergoes a two-electron oxidation mechanism for its peroxidase function. However, subsequent work revealed that the 4-IP internal binding site is actually an inhibitor binding site: both 4-IP and 4-BP function as inhibitors to DHP's peroxidase function.^{15,16} Moreover, ¹H–¹⁵N heteronuclear single quantum coherence experiments show that inhibitor 4-bromophenol (4-BP) and substrate 2,4,6-trichlorophenol

(2,4,6-TCP) induce chemical shift deviation at different regions of DHP upon the titration.³⁰ 4-BP induces the largest chemical shift perturbation for hydrophobic residues in the distal pocket, whereas 2,4,6-TCP causes the largest chemical shift deviation on distal histidine H55 and residues near the dimer interface. Moreover, flow-EPR experiments showed that DHP would produce isotropic a 2,4,6-TCP radical intermediate that could exist only in bulk solution, which strongly supports an external substrate binding site on the protein surface where the substrate is converted to the corresponding radical intermediate by a one-electron oxidation mechanism, as observed in other classical heme peroxidases.²⁹

The inhibitor and substrate have distinct binding sites in DHP, but their binding is mutually exclusive because of the requirement for position switching by the distal histidine (H55), which is a unique feature of the enzyme.¹⁵ Two X-ray crystal structures solved recently show that substrates 2,4,6-TCP and 2,4,6-TBP also have binding sites buried deeply inside the globin at the α -edge of the heme.^{16,20} This type of binding site is unique to DHP and has not been observed in heme peroxidases or other globins. Kinetic study has shown that 2,4,6-TCP and 2,4,6-TBP cause substrate inhibition at high substrate concentration, which suggests that internal binding may provide the explanation for substrate inhibition.¹⁶ One of the X-ray crystallographic studies revealed a second internal mode of binding for 2,4,6-TCP that lies between the inhibitor site and the surface of the protein.^{16,20} The function of this binding site is not clear, but the fact that it exists suggests that the distal pocket (above the heme) is quite large and can accommodate molecules in several different conformations. The fact that the inhibitor binding site is internal indicates that the active substrate binding site for peroxidase function is external, which is consistent with known peroxidase binding sites.³¹ Because there are, at a minimum, three modes of binding known at the present time (two internal and one external), this aspect of DHP structure is consistent with the hypothesis that DHP has multiple functions.

This study reexamines DHP's peroxidase kinetics in light of the relative binding constants determined by a fluoride titration technique, developed previously,³² to map the substrate binding profile in DHP A and DHP B, two isoforms of DHP that differ by five amino acid (I9L, R32K, Y34N, N81S, S91G) and HRP. By applying a two-dimensional kinetic data strategy, we present a graphical and analytical method to better understand DHP's peroxidase kinetic behavior and illustrate the kinetic roles of external and internal substrate binding sites and the interaction between internal binding substrate and cosubstrate H₂O₂. Thus, the kinetic models provide further evidence in support of a peroxidase mechanism and deepen our understanding of the specific interactions of 2,4,6-TBP, which has been considered as a native substrate ever since its discovery in 1996.²

MATERIAL AND METHODS

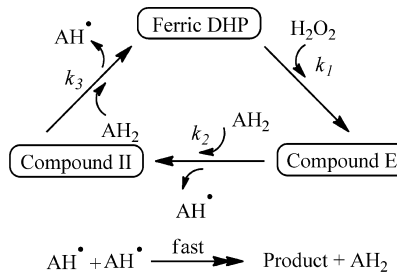
Materials. All the reagents and chemicals were purchased from Sigma-Aldrich and Acros and used without further purification. 2,4,6-Trichlorophenol (2,4,6-TCP) and 2,4,6-tribromophenol (2,4,6-TBP) and 2,2'-azino-bis(3-ethylbenzothiazoline-6-sulfonic acid) (ABTS) were each dissolved in 100 mM, pH = 7.0 potassium phosphate (KP_i) buffer to prepare the substrate stock solutions. Hydrogen peroxide solution was freshly made before each kinetic experiment. A 30% reagent grade hydrogen peroxide (H₂O₂) solution was

added to 100 mM, pH = 7.0 KP_i buffer to make the stock solution. Wild-type His6X DHP A and DHP B were expressed in *Escherichia coli* and purified as previously described.³³ DHP was oxidized by excess K₃[Fe(CN)₆] to reach the ferric state and then filtering through a NAP-2S column to eliminate excess K₃[Fe(CN)₆]. The concentration of ferric DHP was determined by using the Soret band molar absorption coefficient, $\epsilon_{406\text{nm}} = 116\,400 \text{ M}^{-1} \text{ cm}^{-1}$. Horseradish peroxidase (HRP, EC 1.11.1.7) isoenzyme C (type VI) was purchased from Sigma-Aldrich and used without further purification. The concentration of ferric HRP was determined spectroscopically by using $\epsilon_{403\text{nm}} = 92\,000 \text{ M}^{-1} \text{ cm}^{-1}$.

Bisubstrate Ping-Pong Mechanism for DHP's Peroxidase Function. A peroxidase-catalyzed oxidation reaction generally requires both a substrate and cosubstrate. The substrate is a reducing substrate, AH₂, and the cosubstrate is a peroxide, which can be either H₂O₂ or an organic hydroperoxide. The peroxide reacts with the ferric heme of the peroxidase to form the highly active oxo-ferryl species, compound I/compound ES for the following catalytic oxidation reaction.^{34,35} Subsequently, the peroxidase reaction cycle follows a ping-pong mechanism, which consists of two one-electron transfer steps: (1) a one-electron reduction by reducing substrate, which generates a substrate radical intermediate, and (2) a second one-electron reduction back to the ferric heme, which generates another substrate radical intermediate. The term ping-pong has been used for a range of peroxidases to describe the radical pathway in which both electron transfer steps lead to oxidation of the substrate. When the activation step is included, the cycle consists of the three steps shown in Scheme 1.

$$V_0 = \frac{k_1 k_2 k_3 [E]_0 [\text{H}_2\text{O}_2][\text{AH}_2]}{k_2 k_3 [\text{AH}_2] + k_1(k_2 + k_3)[\text{H}_2\text{O}_2]} \quad (1)$$

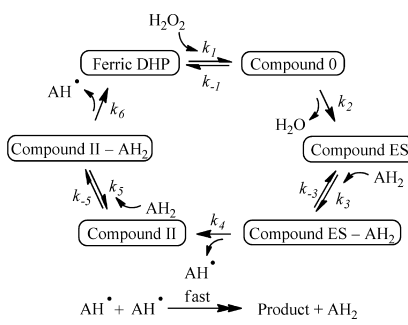
Scheme 1. Original DHP Peroxidase Ping-Pong Mechanism



The initial rate can be expressed as a Michaelis–Menten rate equation for both substrate AH₂ and cosubstrate H₂O₂ dimensions according to Scheme 1; however, the mechanism deviates from the assumptions of Michaelis–Menten theory in that the binding of the cosubstrate to create the ES intermediate is not reversible. Moreover, the mechanism in Scheme 1 assumes that the substrate and cosubstrate react with the enzyme or its transition state independently, which implies that there is no interaction between substrate AH₂ and cosubstrate H₂O₂. Therefore, an explicit bisubstrate ping-pong mechanism that includes the reversible binding of substrate AH₂ and cosubstrate H₂O₂ is proposed as shown in Scheme 2.

Although the formation of the highly active oxo-ferryl intermediate is generally believed to be irreversible, the formation of

Scheme 2. Proposed DHP Peroxidase Bisubstrate Ping-Pong Mechanism with Reversible Substrate Binding



compound 0 does involve the reversible binding of H₂O₂ to the ferric heme, a step that may be impeded by steric hindrance and electrostatic interaction in the distal pocket. Compound 0 has been observed in HRP.³⁶ A similar phenomenon has been observed in DHP in the ferrous form, where H₂O₂ can replace bound O₂ to yield a transient H₂O₂-bound adduct;⁴ however, the ferric compound 0 has not been observed in DHP. On the basis of kinetic Scheme 2, $K_m^{\text{H}_2\text{O}_2}$ and $K_m^{\text{AH}_2}$ are defined explicitly by the microscopic rate constants as shown in eqs 2–5. The initial rate equation (eqs 2 and 6) can also be rearranged to the Michaelis–Menten form in both substrate AH₂ and cosubstrate H₂O₂ dimensions. However, V_m^{app} and K_m^{app} are both dependent on the concentration of the complementary substrate as shown in eqs S6 and S7; therefore, we designed a series of kinetic assays to measure trends of the initial rate, V_0 , by varying the concentrations of both substrate AH₂ and cosubstrate H₂O₂ (eq 1). As a result, we can plot the initial rate as the response to two substrate concentration variables in a three-dimensional (3D) kinetic plot and then fit the data on the kinetic “surface” to obtain the kinetic parameters.

$$V_0 = \frac{k_{\text{cat}}[E]_0 [\text{H}_2\text{O}_2][\text{AH}_2]}{K_m^{\text{H}_2\text{O}_2}[\text{AH}_2] + K_m^{\text{AH}_2}[\text{H}_2\text{O}_2] + [\text{H}_2\text{O}_2][\text{AH}_2]} \quad (2)$$

In which

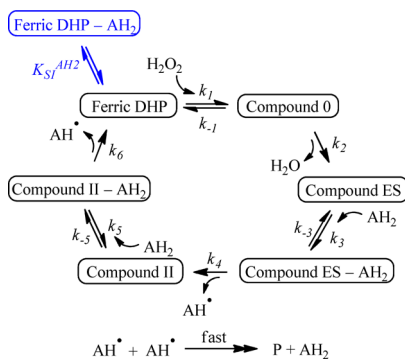
$$k_{\text{cat}} = \frac{k_2 k_4 k_6}{k_4 k_6 + k_2 k_4 + k_2 k_6} \quad (3)$$

$$K_m^{\text{H}_2\text{O}_2} = \frac{(k_{-1} + k_2)k_4 k_6}{(k_4 k_6 + k_2 k_4 + k_2 k_6)k_1} \quad (4)$$

$$K_m^{\text{AH}_2} = \frac{(k_{-3} + k_4)k_1 k_2 k_5 k_6 + (k_{-5} + k_6)k_1 k_2 k_3 k_4}{k_3 k_5 (k_4 k_6 + k_2 k_4 + k_2 k_6)} \quad (5)$$

In Scheme 3, the competitive binding between substrate AH₂ and cosubstrate H₂O₂ in the distal pocket that gives rise to substrate inhibition is included in the initial rate equation (eq 6). The reaction sequence leading to peroxidase chemistry requires that ferric enzyme react with cosubstrate H₂O₂ first to form the active oxoferryl species compound I/compound ES. This mechanism does not rule out the possibility that substrate AH₂ can bind to the ferric enzyme in the distal pocket before H₂O₂ enters. Therefore, a reversible step that 2,4,6-TBP binds to ferric enzyme is included. Substrates that bind internally in the distal pocket will impede H₂O₂'s binding to the heme iron to form the active oxoferryl intermediate for the following catalytic reaction (Scheme 3) because DHP possesses a

Scheme 3. Proposed DHP Peroxidase Bisubstrate Ping-Pong Mechanism Including Substrate AH₂ Inhibition



well-defined internal substrate binding site in the distal pockets observed in several X-ray crystal structures, as shown as an overlay in Figure 1.

$$V_0 = \frac{k_{\text{cat}}[E]_0[H_2O_2][AH_2]}{K_m^{H_2O_2} \left(1 + \frac{[AH_2]}{K_{SI}^{AH_2}} \right) [AH_2] + K_m^{AH_2}[H_2O_2] + [H_2O_2][AH_2]} \quad (6)$$

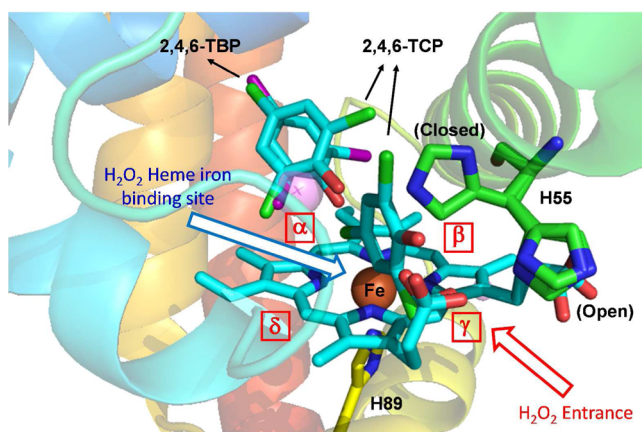


Figure 1. Illustration of two binding modes of two substrates, 2,4,6-TBP and 2,4,6-TCP, in the distal pocket of DHP A obtained from an overlay of the coordinates files from three X-ray crystal structures of the PDB entries 4HF6, 4KMW, and 4KN3.

Bench-Top Mixing Kinetic Assays. The kinetic assays were conducted in 100 mM, pH = 7.0 KP_i buffer using an Agilent 8453 UV-visible spectrophotometer equipped with Peltier temperature controller. The catalytic reactions were carried out in a 0.4 cm path length cuvette from Starna Cells, Inc. with a total volume of 1200 μL. The final enzyme concentration [E]₀ in each sample was 2.4 μM for DHP and 0.2 μM for HRP. All the kinetic assays were conducted at 25 °C. The enzyme and substrate (2,4,6-TCP, 2,4,6-TBP and ABTS) were first mixed in the optical cuvette and placed in the thermal cell to allow them to reach thermal equilibrium (3 min incubation). Subsequently, an aliquot of the H₂O₂ stock solution was added into the cuvette to initiate the reaction. The kinetic data were obtained by monitoring the absorbance at wavelength 272 nm for 2,4,6-TBP, 273 nm for 2,4,6-TCP, and 414 nm for ABTS, which corresponds to the absorbance peaks of the 2,6-dibromoquinone (DBQ), 2,6-dichloroquinone (DCQ), and ABTS cation radical (ABTS^{•+}) products with

extinction coefficients $\epsilon_{272 \text{ nm}} = 14\,000 \text{ M}^{-1} \text{ cm}^{-1}$, $\epsilon_{273 \text{ nm}} = 13\,200 \text{ M}^{-1} \text{ cm}^{-1}$ and, $\epsilon_{414 \text{ nm}} = 31\,100 \text{ M}^{-1} \text{ cm}^{-1}$ respectively.

Fluoride Titration Assays. The fluoride titration experiments were conducted using an Agilent 8453 UV-visible spectrophotometer operating in the standard mode. The titrations were carried out in a 0.2 cm path length cuvette obtained from Starna Cells, Inc. The enzyme concentration, [E]₀, in each sample was 50 μM with a total volume of 600 μL. Substrates (1 mM) were included for the fluoride competitive binding titration, and the cuvette was allowed to incubate for 3 min in the thermal cell to reach thermal equilibrium at 25 °C before the titration, then the fluoride stock solution was gradually titrated in, and the corresponding spectra were recorded. The fluoride titration spectra were eventually normalized according to the protein concentrations in the cuvette. The binding curves were extracted from the spectral region between 300 and 700 nm using singular value decomposition and then fitted into the one-site reversible binding model to obtain the apparent fluoride binding constant K_d^{pp} .

Data Analysis. The initial rate, V_0 , of the kinetic data was calculated on the basis of the method of the initial rate. This consists of a linear fit of the first 5 s of kinetic data collected using the photodiode array spectrophotometer. The V_0 was plotted against the substrate concentration in the substrate dimension and correspondingly against the H₂O₂ concentration in the H₂O₂ dimension. The kinetic data were then fit to the Michaelis-Menten equation to estimate the V_{\max} in the H₂O₂ dimension using Igor Pro 6.10 because no substrate inhibition has been observed in the H₂O₂ dimension in either enzyme. The kinetic data were then plotted in a 3D format, in which the two horizontal axes represent two variables that are substrate AH₂ and cosubstrate H₂O₂ concentrations and the vertical axis shows the responses that are the initial rate. The data were then fitted into eq 2 (without substrate inhibition) or eq 6 (with substrate inhibition) to generate a kinetic rate surface using the multivariate fitting in Wolfram Mathematica 10 to obtain the kinetic parameters that are listed in Tables 1, 2, and 3.

Table 1. Kinetic Parameters Obtained from 2D Michaelis-Menten Kinetics for DHP A

| DHP A | 2,4,6-TCP | 2,4,6-TBP | ABTS |
|----------------------------------|-----------|-----------|-------|
| $k_{\text{cat}} (\text{s}^{-1})$ | 13.67 | 1.83 | 1.05 |
| $K_m^{H_2O_2} (\text{mM})$ | 0.335 | 0.212 | 0.029 |
| $K_m^{AH_2} (\text{mM})$ | 2.07 | 1.02 | 0.448 |

Table 2. Kinetic Parameters Obtained from 2D Michaelis-Menten Kinetics for DHP B

| DHP B | 2,4,6-TCP | 2,4,6-TBP | ABTS |
|----------------------------------|-----------|-----------|-------|
| $k_{\text{cat}} (\text{s}^{-1})$ | 25.72 | 1.87 | 0.70 |
| $K_m^{H_2O_2} (\text{mM})$ | 0.165 | 0.141 | 0.025 |
| $K_m^{AH_2} (\text{mM})$ | 0.685 | 0.312 | 0.229 |
| $K_{SI}^{AH_2} (\text{mM})$ | 0.325 | 1.34 | |

RESULTS

The data will first be presented as rate profiles along both the substrate and cosubstrate concentration dimensions and subsequently as 3D surfaces showing both concentration dependences in a single plot. Because the rate depends on both the substrate and cosubstrate, we can refer to them as

Table 3. Kinetic Parameters Obtained from 2D Michaelis-Menten Kinetics for HRP

| HRP | 2,4,6-TCP | 2,4,6-TBP | ABTS ³⁷ |
|--------------------------------------|-----------|-----------|--------------------|
| k_{cat} (s^{-1}) | 571.3 | 223.4 | 52.5 |
| $K_m^{\text{H}_2\text{O}_2}$ (mM) | 0.050 | 0.093 | 0.012 |
| $K_m^{\text{AH}_2}$ (mM) | 5.40 | 4.53 | 5.1 |

complementary “substrates”, despite the fact that H_2O_2 is most often referred to as a cosubstrate. Starting with the standard 2D representation, Figure 2 shows the plots of the initial rate of the DHP A-catalyzed peroxidase reaction against the substrate 2,4,6-TCP concentration (0–1600 μM) and cosubstrate H_2O_2 concentration (0–2400 μM). It is evident that the initial rate increases proportionally to the respective concentration, either 2,4,6-TCP or H_2O_2 , and then levels off at a sufficiently high concentration. However, under certain conditions, there is a reduction in the rate at the highest 2,4,6-TCP substrate concentrations. This trend is most obvious for 2,4,6-TCP when the H_2O_2 concentration is kept constant at 100 μM . A similar kinetic pattern can be observed for substrate 2,4,6-TBP with the added observation that the rate decreases for a very high 2,4,6-TBP concentration, as shown in Figures 2 and S1. The tendency of the rate to decrease at a high 2,4,6-TXP concentration is observed in both DHP A and B. The kinetic data show that the mutual effects of complementary substrates on the initial rate can be predicted by eqs S6 and S7, based on the model described in Scheme 3. The decrease in rate at high 2,4,6-TXP concentration is predicted by the model that includes the effect of substrate inhibition. Substrate inhibition is observed most prominently at low H_2O_2 concentration in the 2,4,6-TCP kinetics, in agreement with the model. No cosubstrate inhibition has been observed in the H_2O_2 dimension, even when the H_2O_2 concentration is up to 1000-fold greater than the enzyme concentration. Similar substrate inhibition kinetic patterns have also been observed for substrate 2,4,6-TBP. DHP B shows the same trends as DHP A (Figure 3).

The kinetic parameters listed in Tables 1 and 3 show that both DHP A and DHP B have higher catalytic rates for oxidation of 2,4,6-TCP than of 2,4,6-TBP, but unlike the native substrate 2,4,6-TBP, 2,4,6-TCP causes a more severe substrate inhibition than 2,4,6-TBP because its $K_{\text{SI}}^{\text{AH}_2}$ is ~50% of its $K_m^{\text{AH}_2}$. The substrate inhibition produced by 2,4,6-TXP (X = Cl, Br) is presumably due to the internal binding in the distal pocket in a position that is observed in the crystal structure,^{15,17} in which the substrate either blocks the H_2O_2 heme iron axial position for H_2O_2 to form compound 0 or impedes the entering of H_2O_2 into the distal pocket.

A well-studied peroxidase substrate, ABTS, was also used to test DHP’s peroxidase function.^{37,38} As a typical peroxidase reducing substrate, ABTS is first oxidized to form ABTS⁺ by losing one electron. Further one-electron oxidation produces ABTS²⁺. Because ABTS has a much larger molecular size than that of 2,4,6-TCP and 2,4,6-TBP, it is much less likely to bind internally in the distal pocket in DHP, which implies that no substrate inhibition should be observed for ABTS (Figure 4). Indeed, we have not observed any decline in the initial rate, even when the ABTS concentration is as high as 4 mM, which is ~1600-fold greater than the enzyme concentration in the kinetic assay. Moreover, because ABTS does not block H_2O_2 entrance, its $K_m^{\text{H}_2\text{O}_2}$ is ~1/6–1/10 that of 2,4,6-TXP (X = Cl, Br), which indicates a much higher H_2O_2 binding affinity.

The peroxidase function of DHP was also compared with that of HRP using the same ping-pong mechanism kinetic scheme.^{37,38} In the present study, we have included the complete 2D kinetic analysis for HRP using substrates 2,4,6-TCP and 2,4,6-TBP. Apparently, HRP has much higher catalytic rate (~20–120-fold) than that of DHP in terms of its peroxidase function; however, its $K_m^{\text{AH}_2}$ is ~3–20-fold larger than that of DHP, suggesting much weaker substrate binding on the protein surface for HRP. Moreover, no substrate inhibition has been observed for any of these three substrates in HRP. Even at very low H_2O_2 concentration (20 μM), the initial rate does not decline when the 2,4,6-TCP concentration is increased to 3600 μM , as shown in Figures S3 and S4. As for 2,4,6-TBP, the

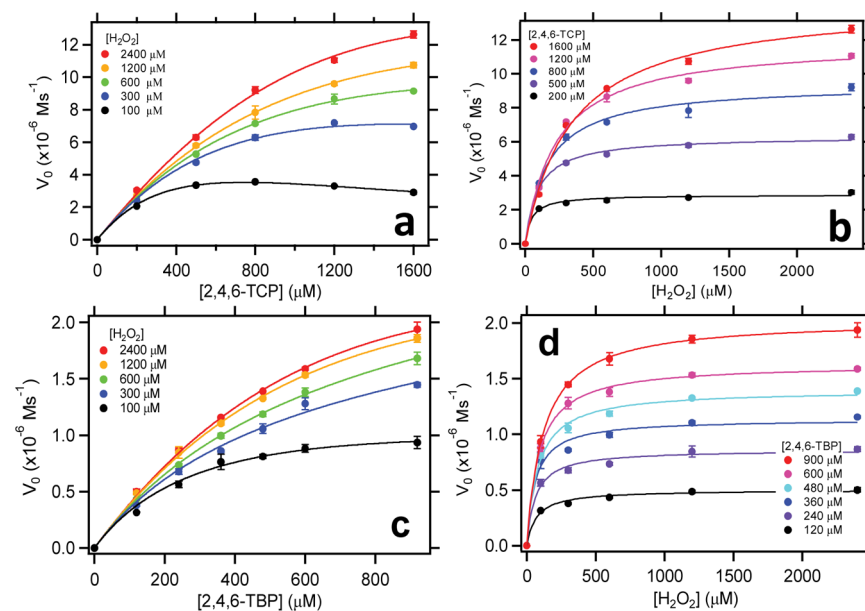


Figure 2. Kinetics of DHPA (2.4 μM)-catalyzed oxidation of 2,4,6-TCP or 2,4,6-TBP in the presence of H_2O_2 . (a) 2,4,6-TCP dimension, (b) H_2O_2 dimension (with 2,4,6-TCP), (c) 2,4,6-TBP dimension, (d) H_2O_2 dimension (with 2,4,6-TBP) in the 100 mM KP_i buffer at pH 7.0.

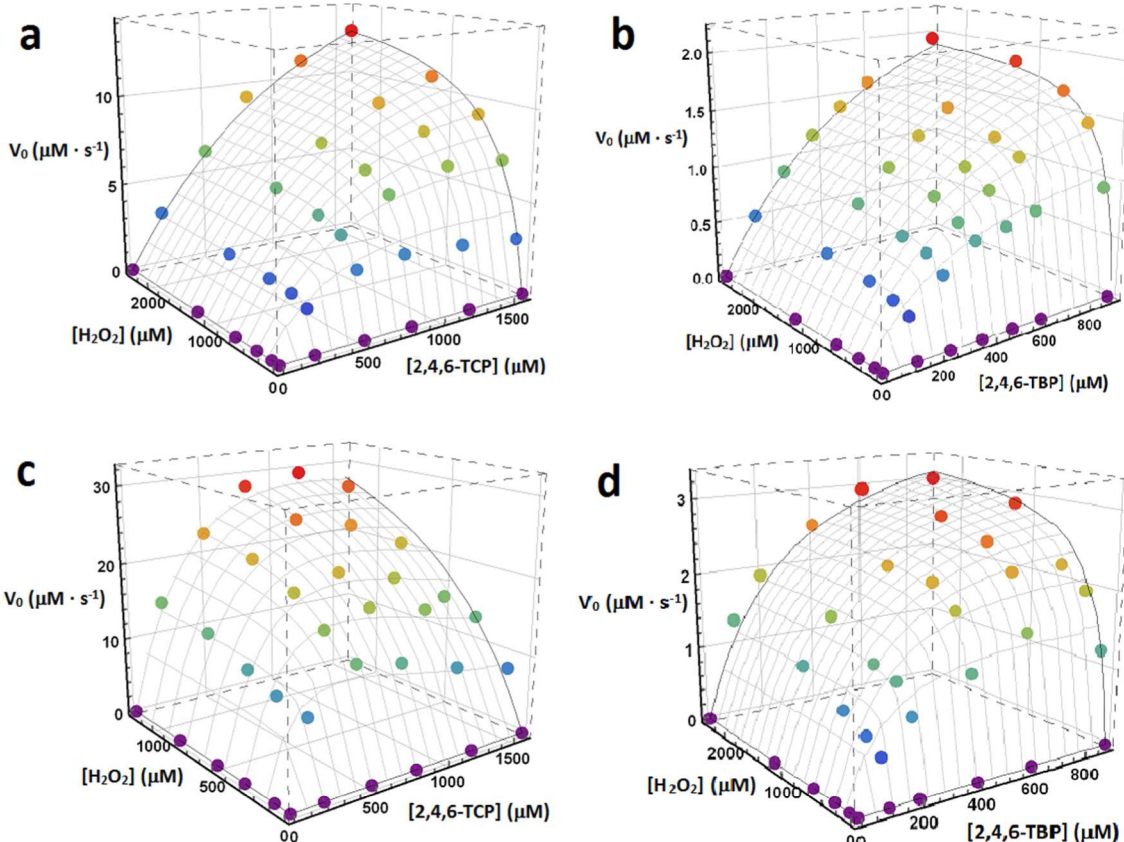


Figure 3. 3D plot of kinetics of DHP ($2.4 \mu\text{M}$) catalyzed oxidation of 2,4,6-TXP ($\text{X} = \text{Cl}, \text{Br}$) in the presence of H_2O_2 . (a) DHP A with 2,4,6-TCP; (b) DHP A with 2,4,6-TBP; (c) DHP B with 2,4,6-TCP; (d) DHP B with 2,4,6-TBP.

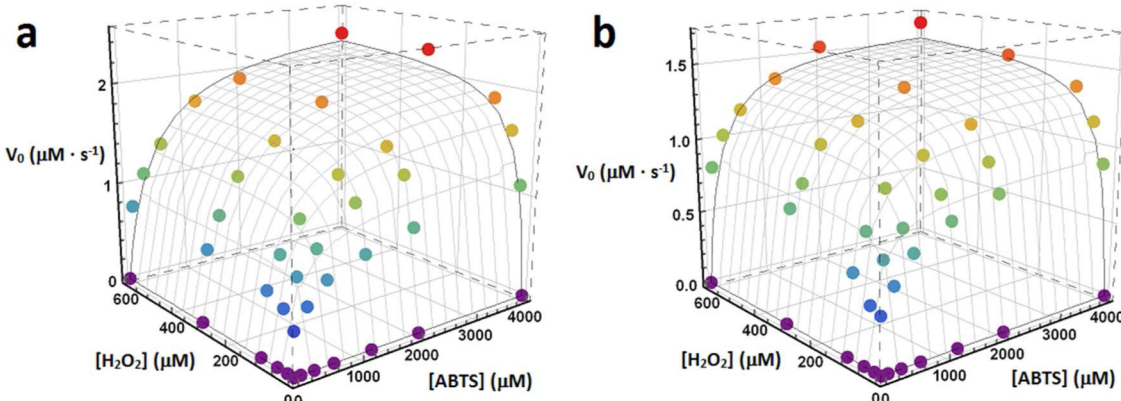


Figure 4. 3D plot of kinetics of DHP ($2.4 \mu\text{M}$) catalyzed oxidation of ABTS in the presence of H_2O_2 . (a) DHP A with ABTS; (b) DHP B with ABTS.

kinetic measurement is limited by its solubility in aqueous solution and its denaturing effect. HRP precipitates by the end of the kinetic assay for concentrations of $2,4,6\text{-TBP} > 900 \mu\text{M}$; therefore, HRP's kinetic profile is consistent with surface substrate binding that is distant from the distal pocket and heme Fe. Stability and folding studies show that DHP is much more resistant to precipitation by 2,4,6-TXP.²³

The fluoride titration experiments clearly show that DHP A (Figure 5) and HRP have different substrate binding profiles. During the titration, the fluoride anion will bind to heme Fe to form the 6-coordinated high-spin (6cHS) heme–fluoride adduct, which is indicated by the charge transfer band CT₁

at 605 nm for DHP and 611 nm for HRP, as shown in Figure 6. In the absence of any substrate, the fluoride anion dissociation constants are denoted as K_d^f . In the presence of substrate, we denote the apparent fluoride dissociation constant as K_d^{app} . Equation S8, which describes the quantitative relationship of K_d^{app} in terms of K_d^f and substrate concentration $[L]$, is given in the Supporting Information. As a result, the fluoride binding affinity might become much lower because of the steric hindrance exerted by internal substrate binding. Competitive binding of this type has been demonstrated for substrates 2,4,6-TBP and 2,4,6-TCP in DHP A. The K_d^{app} increases ~ 5 fold and ~ 3 fold, respectively, indicating the weaker binding

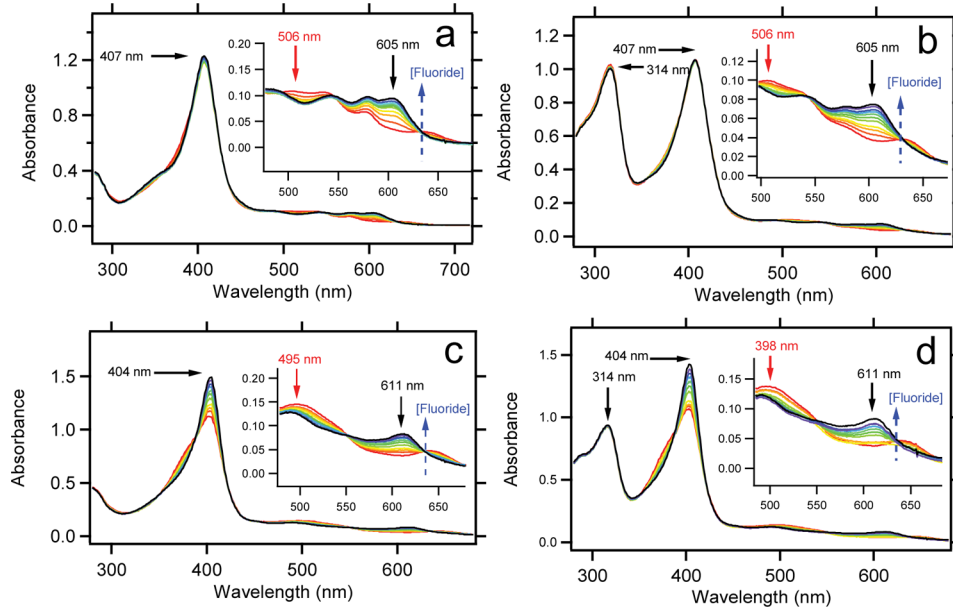


Figure 5. UV-vis spectra of fluoride titration of WT DHP A (a) in the absence or (b) in the presence of 1 mM 2,4,6-TBP and HRP (c) in the absence or (d) in the presence of 1 mM 2,4,6-TBP in the 100 mM KP_i buffer at pH 7.0.

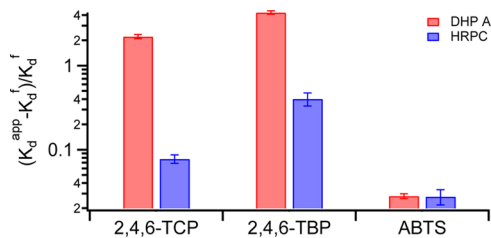


Figure 6. Fluoride titration profile of DHP A and HRP in the presence of substrate: 2,4,6-TCP, 2,4,6-TBP, and ABTS.

Table 4. Apparent Fluoride Dissociation Constant K_d^{app} of DHPA and HRP with or without Substrates

| K_d^{app} (mM) | DHP A | HRP |
|-------------------------|----------------|-----------------|
| protein (K_d^f) | 4.5 ± 0.1 | 69.5 ± 4.8 |
| +1 mM 2,4,6-TCP | 14.5 ± 0.8 | 74.9 ± 6.9 |
| +1 mM 2,4,6-TBP | 23.8 ± 1.0 | 97.4 ± 15.7 |
| +1 mM ABTS | 4.6 ± 0.3 | 71.4 ± 13.8 |

affinity of the fluoride anion, whereas for HRP, K_d^{app} increases only ~40% and ~8%, respectively, showing that both 2,4,6-TBP and 2,4,6-TCP have much weaker interactions with the fluoride anion, which suggests a likely external binding at HRP. Substrate ABTS shows a very small effect on the fluoride binding affinity for both DHP A and HRP. Because of the much larger molecular size of ABTS compared with 2,4,6-TBP, ABTS has very little possibility to bind internally in the distal pocket in both DHP and HRP; therefore, the ABTS binding site must be located on the protein surface of both proteins.

The fluoride titration experiments are consistent with two modes of binding for 2,4,6-TCP and 2,4,6-TBP. The fact that competitive binding with fluoride is observed indicates that internal binding of 2,4,6-TCP and 2,4,6-TBP in DHP does occur; however, the binding is sufficiently weak that it is consistent with the existence of an external substrate binding site for DHP at a low concentration of 2,4,6-TCP and 2,4,6-TBP, which is needed for DHP to carry out its peroxidase function.

The fluoride titration result for HRP shows the much weaker interactions between substrates and heme-bound fluoride anion (Table 4). This result suggests that there is no internal binding of substrates, which is consistent with the lack of substrate inhibition in HRP. This evidence leads us to suggest that the substrates 2,4,6-TXP bind at the δ -edge of the heme, like other aromatic substrates of HRP.^{31,39}

DISCUSSION

The Significance of External and Internal Substrate Binding Sites. The substrate inhibition observed in the DHP kinetics gives new insight into the internal binding site of 2,4,6-TBP and 2,4,6-TCP observed in the X-ray crystal structures.^{16,20} These structures provide the first α -edge substrate binding site observed in any heme peroxidase. Normally, the substrate either binds at the heme δ -edge in the BHA binding sites in HRP or binds at the γ -edge of the heme, where propionate groups would play an important role in stabilizing the substrate binding.³¹ Therefore, it was a surprise to find that DHP possess a deeply buried substrate binding site for 2,4,6-TCP/2,4,6-TBP on the α -edge of the heme.^{16,20} Although the data presented here suggest that this binding site is an inhibitor binding site for peroxidase function, the main function of the binding site may relate to one of the other functions that has been recently discovered. For example, the peroxygenase function involves oxygen atom transfer and requires a substrate binding site very close to the heme Fe.⁷ Our working hypothesis for DHP function suggests that the internal binding binding site is primarily a 2,4-dibromophenol (2,4-DBP) substrate binding site for peroxygenase function, but happens also to give rise to substrate inhibition for very high 2,4,6-TXP concentration.

A further hypothesis is that DHP A and B have external binding sites for the peroxidase function, which would make them similar to HRP in that respect. Flow-EPR experiments suggest that the primary functional binding of 2,4,6-TBP is external to the protein on the basis of the detected 2,4,6-trichlorophenoxy radical intermediate.²⁹ The phenoxy radical

can be observed only if the substrate rapidly dissociates from the protein and then flows through the EPR flat cell used in the experiment. Evidence for radicals can be found in both the EPR spectra and the secondary products, such as 3-hydroxy-2,6-dichloroquinone.⁴⁰ The isotropic character of the EPR spectra also shows that the radical is not associated with a high-molecular-weight protein, but rather, is free to react in bulk solution.²⁹ This would not be consistent with internal binding because an internally bound substrate typically undergoes a direct 2-electron peroxidase oxidation reaction without involving a substrate radical intermediate. The kinetic data obtained using ABTS as a substrate further validates the hypothesis that the peroxidase mechanism in DHP A and B involves an external substrate binding site. The large size of ABTS prohibits substrate inhibition observed with the substrates 2,4,6-TCP and 2,4,6-TBP. These results seem to suggest that the internal binding site and substrate inhibition by 2,4,6-TXP may be adventitious and the main binding is on the protein surface.

The result from a previous fluoride competitive binding assay suggests that the internal α -edge site may be the substrate binding site for 2,4-DBP.³² Consistent with this interpretation, the fluoride competitive binding assay shows that 2,4-DBP has a much tighter binding affinity than 2,4,6-TBP in the distal pocket. Therefore, we hypothesize that the α -edge internal substrate binding site of DHP evolved for DHP to carry out to a peroxygenase function for another native substrate, 2,4-DBP, but it may also become a trap for 2,4,6-TBP in the distal pocket at sufficiently high substrate concentration and thereby result in substrate inhibition.

Kinetic Comparison between DHP and HRP: The Tortoise and the Hare. On the basis of numerous experimental observations, we hypothesize that the multifunctional properties of DHP⁷ are a consequence of the role it plays in detoxification combined with an essential role in O₂ transport.¹ Detoxification in benthic ecosystems is a challenge because of the large number of potentially toxic substrates.^{22,41} The evidence shows that DHP has an interaction with a number of different molecules based on both structural and dynamic observations. It will be of interest to individually examine each substrate and determine the factors that give rise to catalysis.

Specifically, with regard to peroxidase activity, the comparative kinetic study between DHP and HRP gives insight into the structure–function relationship required for efficacy in degradation of 2,4,6-TBP. Apparently, HRP peroxidase is superior to DHP in terms of catalytic rate, k_{cat} , for most of the reducing substrates studied, including 2,4,6-TBP; however, HRP is far from an ideal enzyme for DHP's native substrate 2,4,6-TBP because HRP is destabilized by 2,4,6-TBP. HRP starts to aggregate and precipitate during the catalytic reaction when the 2,4,6-TBP concentration reaches 900 μ M, as shown in Figure S5. This denaturation and inactivation of HRP could be the result of the attack of the phenoxy radical generated during the catalytic reaction.⁴² DHP is like the tortoise that wins the race in the fable by being slow and steady in its pace. From an evolutionary perspective, HRP's peroxidase function would not be suitable for a marine worm such as *A. ornata* to survive in an environment that contains 2,4,6-TBP. Like the hare in the fable, HRP is fast, but it cannot sustain that level of activity because of its sensitivity to denaturation by the substrate. From a bioremediation perspective, HRP needs to be either immobilized^{43,44} or protected by additives⁴⁵ so that it can be used as a stable enzymatic catalyst to treat pollutants that

contain halogenated phenols. Apparently, DHP has evolved a strategy to solve the toxicity problems posed by these substrate by having internal binding sites to regulate its peroxidase function. Previous studies have shown that 4-hydroquinone and 4-bromophenol can inhibit the peroxidase function of DHP by binding at the internal inhibitor binding site.^{32,46}

The multiple binding sites of DHP are unusual, but they are not unique. In fact, DHP is an example of a growing list of proteins that have multiple functions or binding sites. For example, a plant peroxidase isolated from *Chamaerops excelsa* palm tree (CEP) with very strong pH and thermal stability also possesses significant substrate inhibition kinetic behavior, which possibly can be attributed to the existence of two substrate binding sites.^{47,48} Current work extends structural studies that suggest that the substrates 2,4,6-TCP and 2,4,6-TBP inhibit DHP's peroxidase function by substrate inhibition at high substrate concentration, which prevents the collapse of the protein stability during the catalytic reaction at high substrate concentration. In conclusion, substrate inhibition of the 2,4,6-TCP and 2,4,6-TBP distinguish the peroxidase function of DHP from that of HRP. The internal substrate binding due to the existence of a large distal pocket above the heme in DHP plays a critical role in regulating the peroxidase function of DHP by substrate inhibition.

ASSOCIATED CONTENT

Supporting Information

The Supporting Information is available free of charge on the ACS Publications website at DOI: 10.1021/acs.jpcb.5b07126.

Derivation of the initial rate equations based on the bisubstrate ping-pong mechanism, other 2D and 3D plots of DHP and HRPC kinetics, equation for apparent fluoride binding affinity (PDF)

AUTHOR INFORMATION

Corresponding Author

*E-mail: franzen@ncsu.edu.

Notes

The authors declare no competing financial interest.

ACKNOWLEDGMENTS

This work was supported by Army Research Office Grant 57861-LS. We thank Zhejiang University and the Guangbiao Scholars Program for partial support of this work.

REFERENCES

- (1) Weber, R. E.; Mangum, C.; Steinman, H.; Bonaventura, C.; Sullivan, B.; Bonaventura, J. Hemoglobins of Two Terebellid Polychaetes: *Enoplobranchus Sanguineus* and *Amphitrite ornata*. *Comp. Biochem. Phys. A* **1977**, *56*, 179–187.
- (2) Chen, Y. P.; Woodin, S. A.; Lincoln, D. E.; Lovell, C. R. An Unusual Dehalogenating Peroxidase from the Marine Terebellid Polychaete *Amphitrite ornata*. *J. Biol. Chem.* **1996**, *271*, 4609–4612.
- (3) Franzen, S.; Thompson, M. K.; Ghiladi, R. A. The Dehaloperoxidase Paradox. *Biochim. Biophys. Acta, Proteins Proteomics* **2012**, *1824*, 578–588.
- (4) D'Antonio, J.; Ghiladi, R. A. Reactivity of Deoxy- and Oxyferrous Dehaloperoxidase B from *Amphitrite ornata*: Identification of Compound II and Its Ferrous–Hydroperoxide Precursor. *Biochemistry* **2011**, *50*, 5999–6011.
- (5) Davydov, R.; Osborne, R. L.; Shanmugam, M.; Du, J.; Dawson, J. H.; Hoffman, B. M. Probing the Oxyferrous and Catalytically Active Ferryl States of *Amphitrite ornata* Dehaloperoxidase by Cryoreduction

- and EPR/ENDOR Spectroscopy. Detection of Compound I. *J. Am. Chem. Soc.* **2010**, *132*, 14995–15004.
- (6) Du, J.; Sono, M.; Dawson, J. H. Functional Switching of *Amphitrite ornata* Dehaloperoxidase from O-2-Binding Globin to Peroxidase Enzyme Facilitated by Halophenol Substrate and H₂O₂. *Biochemistry* **2010**, *49*, 6064–6069.
- (7) Barrios, D. A.; D'Antonio, J.; McCombs, N. L.; Zhao, J.; Franzen, S.; Schmidt, A. C.; Sombers, L. A.; Ghiladi, R. A. Peroxygenase and Oxidase Activities of Dehaloperoxidase-Hemoglobin from *Amphitrite ornata*. *J. Am. Chem. Soc.* **2014**, *136*, 7914–7925.
- (8) Kvist, M.; Ryabova, E.; Nordlander, E.; Bülow, L. An investigation of the Peroxidase Activity of Vitreoscilla Hemoglobin. *JBIC, J. Biol. Inorg. Chem.* **2007**, *12*, 324–334.
- (9) George, P.; Irvine, D. H. Reaction of Metmyoglobin with Hydrogen Peroxide. *Nature* **1951**, *168*, 164–165.
- (10) Lebioda, L. The honorary enzyme hemoglobin turns out to be a real enzyme. *Cell. Mol. Life Sci.* **2000**, *57*, 1817–1819.
- (11) Wan, L.; Twitchett, M. B.; Eltis, L. D.; Mauk, A. G.; Smith, M. In vitro evolution of horse heart myoglobin to increase peroxidase activity. *Proc. Natl. Acad. Sci. U. S. A.* **1998**, *95* (22), 12825–12831.
- (12) Ozaki, S.-i.; Matsui, T.; Watanabe, Y. Conversion of Myoglobin into a Highly Stereo-specific Peroxygenase by the L29H/H64L Mutation. *J. Am. Chem. Soc.* **1996**, *118*, 9784–9785.
- (13) Lin, Y.; Wang, J.; Lu, Y. Functional tuning and expanding of myoglobin by rational protein design. *Sci. China: Chem.* **2014**, *57*, 346–355.
- (14) Ordway, G. A.; Garry, D. J. Myoglobin: An Essential Hemoprotein in Striated Muscle. *J. Exp. Biol.* **2004**, *207*, 3441–3446.
- (15) Thompson, M. K.; Davis, M. F.; de Serrano, V.; Nicoletti, F. P.; Howes, B. D.; Smulevich, G.; Franzen, S. Internal Binding of Halogenated Phenols in Dehaloperoxidase-Hemoglobin Inhibits Peroxidase Function. *Biophys. J.* **2010**, *99*, 1586–1595.
- (16) Zhao, J.; de Serrano, V.; Zhao, J. J.; Le, P.; Franzen, S. Structural and Kinetic Study of an Internal Substrate Binding Site in Dehaloperoxidase-Hemoglobin A from *Amphitrite ornata*. *Biochemistry* **2013**, *52*, 2427–2439.
- (17) De Serrano, V.; Franzen, S. Structural Evidence for Stabilization of Inhibitor Binding by a Protein Cavity in the Dehaloperoxidase-Hemoglobin from *Amphitrite ornata*. *Biopolymers* **2012**, *98*, 27–35.
- (18) Davis, M. F.; Gracz, H.; Vendeix, F. A. P.; de Serrano, V.; Somasundaram, A.; Decatur, S. M.; Franzen, S. Different Modes of Binding of Mono-, Di-, and Trihalogenated Phenols to the Hemoglobin Dehaloperoxidase from *Amphitrite ornata*. *Biochemistry* **2009**, *48*, 2164–2172.
- (19) de Serrano, V.; Chen, Z. X.; Davis, M. F.; Franzen, S. X-ray Crystal Structural Analysis of the Binding Site in the Ferric and Oxyferrous forms of the Recombinant Heme Dehaloperoxidase Cloned from *Amphitrite ornata*. *Acta Crystallogr., Sect. D: Biol. Crystallogr.* **2007**, *63*, 1094–1101.
- (20) Wang, C.; Lovelace, L. S.; Sun, S.; Dawson, J. H.; Lebioda, L. Complexes of Dual-Function Hemoglobin/Dehaloperoxidase with Substrate 2,4,6-Trichlorophenol Are Inhibitory and Indicate Binding of Halophenol to Compound I. *Biochemistry* **2013**, *52*, 6203–6210.
- (21) Lebioda, L.; LaCount, M. W.; Zhang, E.; Chen, Y. P.; Han, K.; WHilton, M. M.; Lincoln, D. E.; Woodin, S. A. An Enzymatic Globin from a Marine Worm. *Nature* **1999**, *401*, 445.
- (22) Fielman, K. T.; Woodin, S. A.; Walla, M. D.; Lincoln, D. E. Widespread Occurrence of Natural Halogenated Organics among Temperate Marine Infauna. *Mar. Ecol.: Prog. Ser.* **1999**, *181*, 1–12.
- (23) Le, P.; Zhao, J.; Franzen, S. Correlation of Heme Binding Affinity and Enzyme Kinetics of Dehaloperoxidase. *Biochemistry* **2014**, *53*, 6863–6877.
- (24) Dunford, H. B. *Peroxidases in Chemistry and Biology* Vol. 2 (Everse, J., Everse, K. E., & Grisham, M. B., Eds) CRC Press, Boca Raton, FL, 1991, 1–24.
- (25) Bakovic, M.; Dunford, H. B. Intimate Relation between the Cyclooxygenase and Peroxidase Activities of Prostaglandin H Synthase - Peroxidase Reaction of Ferulic Acid and its Influence on the Reaction of Arachidonic Acid. *Biochemistry* **1994**, *33*, 6475–6482.
- (26) Belyea, J.; Gilvey, L. B.; Davis, M. F.; Godek, M.; Sit, T. L.; Lommel, S. A.; Franzen, S. Enzyme Function of the Globin Dehaloperoxidase from Amphitrite Ornata is Activated by Substrate Binding. *Biochemistry* **2005**, *44*, 15637–15644.
- (27) Osborne, R. L.; Taylor, L. O.; Han, K. P.; Ely, B.; Dawson, J. H. Amphitrite Ornata Dehaloperoxidase: Enhanced Activity for the Catalytically Active Globin using MCPBA. *Biochem. Biophys. Res. Commun.* **2004**, *324*, 1194–1198.
- (28) Ferrari, R. P.; Laurenti, E.; Trotta, F. Oxidative 4-Decoloration of 2,4,6-Trichlorophenol Catalyzed by Horseradish Peroxidase. *JBIC, J. Biol. Inorg. Chem.* **1999**, *4*, 232–237.
- (29) Sturgeon, B. E.; Battenburg, B. J.; Lyon, B. J.; Franzen, S. Revisiting the Peroxidase Oxidation of 2,4,6-Trihalophenols: ESR Detection of Radical Intermediates. *Chem. Res. Toxicol.* **2011**, *24*, 1862–1868.
- (30) Davis, M. F.; Bobay, B. G.; Franzen, S. Determination of Separate Inhibitor and Substrate Binding Sites in the Dehaloperoxidase-Hemoglobin from *Amphitrite ornata*. *Biochemistry* **2010**, *49*, 1199–1206.
- (31) Gumiero, A.; Murphy, E. J.; Metcalfe, C. L.; Moody, P. C. E.; Raven, E. L. An Analysis of Substrate Binding Interactions in the Heme Peroxidase Enzymes: A Structural Perspective. *Arch. Biochem. Biophys.* **2010**, *500*, 13–20.
- (32) Zhao, J.; Franzen, S. Kinetic Study of the Inhibition Mechanism of Dehaloperoxidase-Hemoglobin A by 4-Bromophenol. *J. Phys. Chem. B* **2013**, *117*, 8301–8309.
- (33) Ma, H.; Thompson, M. K.; Gaff, J.; Franzen, S. Kinetic Analysis of a Naturally Occurring Bioremediation Enzyme: Dehaloperoxidase-hemoglobin from *Amphitrite ornata*. *J. Phys. Chem. B* **2010**, *114*, 13823–13829.
- (34) Dunford, H. B.; Stillman, J. S. On the Function and Mechanism of Action of Peroxidases. *Coord. Chem. Rev.* **1976**, *19*, 187–251.
- (35) Poulos, T. L.; Kraut, J. The Stereochemistry of Peroxidase Catalysis. *J. Biol. Chem.* **1980**, *255*, 8199–8205.
- (36) Baek, H. K.; Van Wart, H. E. Elementary Steps in the Formation of Horseradish Peroxidase Compound I: Direct Observation of Compound 0, a New Intermediate with a Hyperporphyrin Spectrum. *Biochemistry* **1989**, *28*, 5714–5719.
- (37) Rodriguez-Lopez, J. N.; Smith, A. T.; Thorneley, R. N. F. Role of Arginine 38 in Horseradish Peroxidase: A Critical Residue for Substrate Binding and Catalysis. *J. Biol. Chem.* **1996**, *271*, 4023–4030.
- (38) Rodriguez-Lopez, J. N.; Gilabert, M. A.; Tudela, J.; Thorneley, R. N. F.; Garcia-Cánovas, F. Reactivity of Horseradish Peroxidase Compound II toward Substrates: Kinetic Evidence for a Two-Step Mechanism†. *Biochemistry* **2000**, *39*, 13201–13209.
- (39) Henriksen, A.; Smith, A. T.; Gajhede, M. The Structures of the Horseradish Peroxidase C-Ferulic Acid Complex and the Ternary Complex with Cyanide Suggest How Peroxidases Oxidize Small Phenolic Substrates. *J. Biol. Chem.* **1999**, *274*, 35005–35011.
- (40) Franzen, S.; Sasan, K.; Sturgeon, B. E.; Lyon, B. J.; Battenburg, B. J.; Gracz, H.; Dumariah, R.; Ghiladi, R. Nonphotochemical Base-Catalyzed Hydroxylation of 2,6-Dichloroquinone by H₂O₂ Occurs by a Radical Mechanism. *J. Phys. Chem. B* **2012**, *116*, 1666–1676.
- (41) Lincoln, D. E.; Fielman, K. T.; Marinelli, R. L.; Woodin, S. A. Bromophenol Accumulation and Sediment Contamination by the Marine Annelids *Notomastus lobatus* and *Thelepus crispus*. *Biochem. Syst. Ecol.* **2005**, *33*, 559–570.
- (42) Huang, Q.; Huang, Q.; Pinto, R. A.; Griebenow, K.; Schweitzer-Stenner, R.; Weber, W. J. Inactivation of Horseradish Peroxidase by Phenoxyl Radical Attack. *J. Am. Chem. Soc.* **2005**, *127*, 1431–1437.
- (43) Alemzadeh, I.; Nejati, S. Phenols Removal by Immobilized Horseradish Peroxidase. *J. Hazard. Mater.* **2009**, *166*, 1082–1086.
- (44) Huang, J.; Chang, Q.; Ding, Y.; Han, X.; Tang, H. Catalytic Oxidative Removal of 2,4-Dichlorophenol by Simultaneous use of Horseradish Peroxidase and Graphene Oxide/Fe₃O₄ as Catalyst. *Chem. Eng. J.* **2014**, *254*, 434–442.
- (45) Wu, Y.; Taylor, K. E.; Biswas, N.; Bewtra, J. K. A model for the Protective Effect of Additives on the Activity of Horseradish

Peroxidase in the Removal of Phenol. *Enzyme Microb. Technol.* **1998**, *22*, 315–322.

(46) Zhao, J.; Zhao, J.; Franzen, S. The Regulatory Implications of Hydroquinone for the Multifunctional Enzyme Dehaloperoxidase-hemoglobin from Amphitrite Ornata. *J. Phys. Chem. B* **2013**, *117*, 14615–24.

(47) Cuadrado, N. H.; Arellano, J. B.; Calvete, J. J.; Sanz, L.; Zhadan, G. G.; Polikarpov, I.; Bursakov, S.; Roig, M. G.; Shnyrov, V. L. Substrate Specificity of the Chamaerops Excelsa Palm Tree Peroxidase. A Steady-state Kinetic Study. *J. Mol. Catal. B: Enzym.* **2012**, *74*, 103–108.

(48) Bernardes, A.; Textor, L. C.; Santos, J. C.; Cuadrado, N. H.; Kostetsky, E. Y.; Roig, M. G.; Bavro, V. N.; Muniz, J. R. C.; Shnyrov, V. L.; Polikarpov, I. Crystal Structure Analysis of Peroxidase from the Palm Tree Chamaerops Excelsa. *Biochimie* **2015**, *111*, 58–69.